

# Facies Structure and Quantitative Parameters of the Pleistocene Sediments of the Cordilleran Submarine Margin

M. A. Levitan<sup>a, \*</sup>, T. A. Antonova<sup>a</sup>, and A. V. Kol'tsova<sup>a</sup>

<sup>a</sup>*Vernadsky Institute of Geochemistry and Analytical Chemistry, Russian Academy of Sciences,  
ul. Kosygina 19, Moscow, 119991 Russia*

*\*e-mail: m-levitan@mail.ru*

Received December 17, 2018; revised June 19, 2019; accepted September 13, 2019

**Abstract**—The lithological-facies zonality of the Neo- and Eopleistocene sediments from two main areas of the Cordilleran submarine margin is described for the first time. Processing of corresponding maps and isopach schemes using A.B. Ronov's volumetric method made it possible to calculate the quantitative parameters of sedimentation for the distinguished types of Pleistocene sediments. Terrigenous sedimentation predominated and was intensified during the Pleistocene. The accumulation of biogenic opal and carbonates was more intense in the Neopleistocene than in the Eopleistocene.

**Keyword:** bottom sediments, sedimentary basins, Cordilleras, continental slope, shelf, Eopleistocene, Neopleistocene, areas, volumes, dry sediment mass, mass of sediments per time unit, terrigenous turbidites, hemipelagic clays, diatom clays, nanoclays

**DOI:** 10.1134/S0016702920050043

## INTRODUCTION

This paper completes a cycle of our works dedicated to the Pleistocene sediments from the Pacific submarine margins (Levitan et al., 2018a, 2018b, 2018c, et al.). In this cycle, the Neopleistocene, i.e., Middle and Late Pleistocene ( $Q_{2+3}$ , 0.01–0.80 Ma), and Eopleistocene or Early Pleistocene ( $Q_1$ , 0.80–1.80 Ma according to “old” scale, (Gradstein et al., 2004)) are considered separately.

The above-mentioned publications on the back-arc sedimentary basins of active margins in the northern and western Pacific Ocean, as well as sedimentary basins of the Antarctic passive margin in the southwest were mainly based on the deep-sea drilling results. In this communication, the evolution of Pleistocene sediments of sedimentary basin of the Andean-type active margin in the eastern and northeastern Pacific ocean is described on the basis of materials obtained during DSDP, ODP and IODP legs.

## MODERN SEDIMENTATION ENVIRONMENT

The Cordilleran mountainous belt has tremendous sizes: length of 8 thou. km, width from 700–800 to 1500 km, and height over 6 km. Its evolution lasted for about 750 Ma. Along strike, the Cordilleras are subdivided into four segments, the boundaries between which closely coincide with state boundaries: Alaskan, Canadian, American proper, and Mexican (Khain, 2001). The Cordilleras belong to the mountainous

belts subjected to the most intense modern neotectonic movements (Trifonov and Sokolov, 2015). For instance, the land areas of western Canada (British Columbia) for the last 10 Ma have been raised for 2–4 km, while shelf was submerged (Clague et al., 1982). The Pleistocene is characterized by active volcanic activity, with the most powerful explosive volcanism in Central America.

The Cordilleran submarine margin is a narrow zone of continental shelves and steep slopes, which ended with the Central America deep-water trench in the south (Fig. 1) and subduction zone with deformation front in the north (Fig. 1b).

Owing to submeridional extension and large size, the margin spans several climatic belts: from subarctic belt in the north to the equatorial–tropical belts in the south. The latitudinal zoning also significantly affects the circulation of surface waters with varying temperature characteristics from the north to south. The southern area (from 8° to 18° N) is controlled by the eastward flowing North Equatorial Counter Current and the westward flowing North Equatorial current. The southward flowing Californian Current also plays a definite role (Fig. 1a) (Berger et al., 1987). At the extreme south of the considered area, the average primary production on the submarine margin varies from 200 to 500, and is 100–200 g C/m<sup>2</sup>/y in the north (beyond the influence zone of the Californian Current) (Berger et al., 1987).

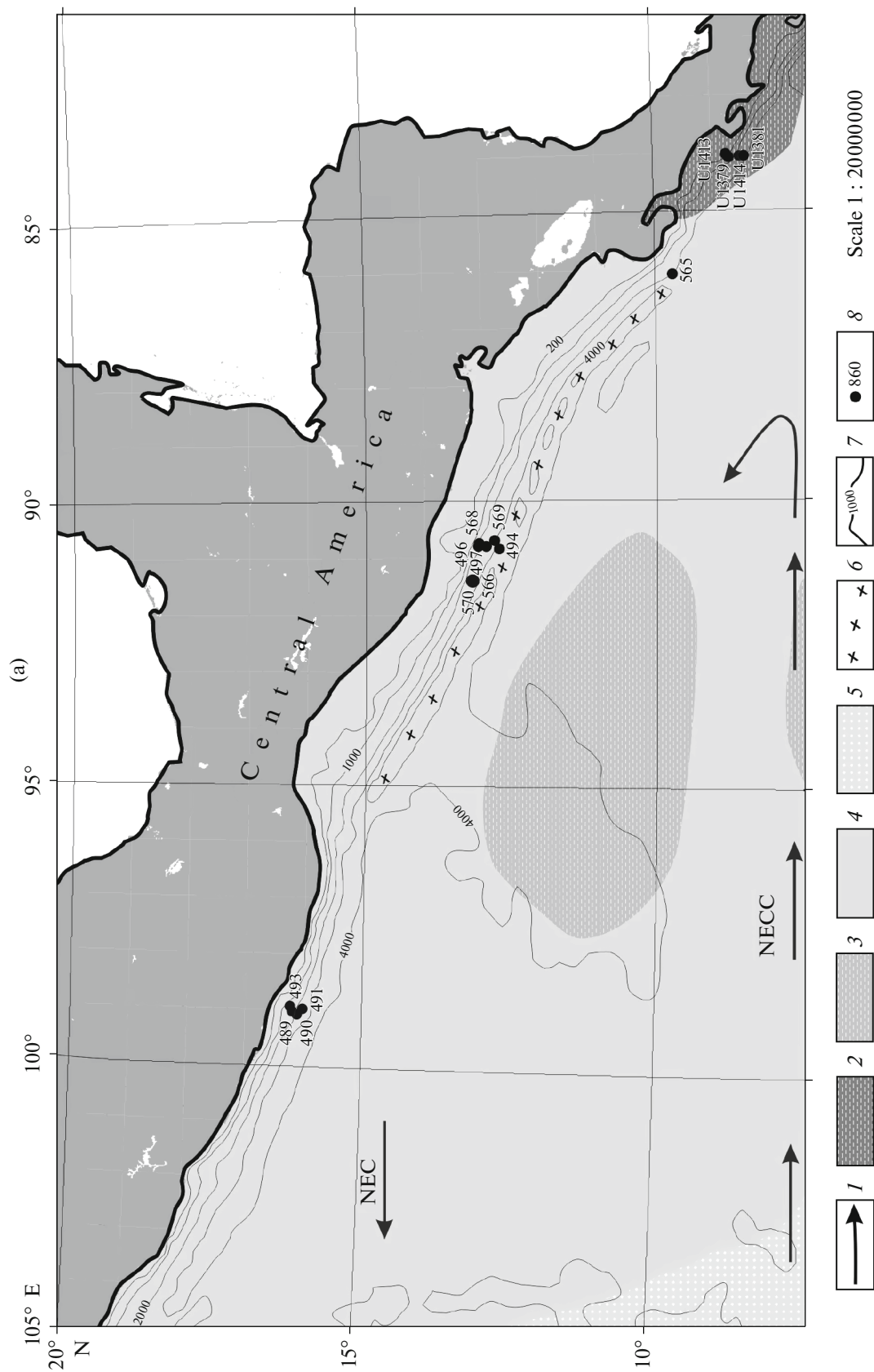


**Fig. 1.** Position of deep-sea drilling holes on the Cordilleran submarine margin ((a) southern area, (b) northern area). Symbols in Fig. 1a: (1) surface currents (Berger et al., 1987) (NECC) Northern Equatorial Counter Current); (NEC) Northern Equatorial Current); (2–5) average annual primary production (Berger et al., 1987) (2) 200–500; (3) 100–200; (4) 60–100; (5) 35–60  $\text{g C/m}^2/\text{y}$ ); (6) Mid–American deep-water trench; (7) isobaths (in m); (8) deep-sea drilling hole numbers. Symbols for Fig. 1b: (1) surface current (Lopes et al., 2010) ((AC) Alaskan Current; (CC) Californian Current); (2) subduction zone; (3) Astoria, (4) Eel River basin; (5) Nitinat; (3) Nitinat; (3) Nitinat; (5) numbers of fans ((1) Alaska Bay, (2) Nitinat; (3) Nitinat; (3) Nitinat; (5) Santa Monica basin) (Westbrook et al., 1994; Lyle et al., 1997; Whitmarsh et al., 1997); (6) deep-sea drilling hole numbers.

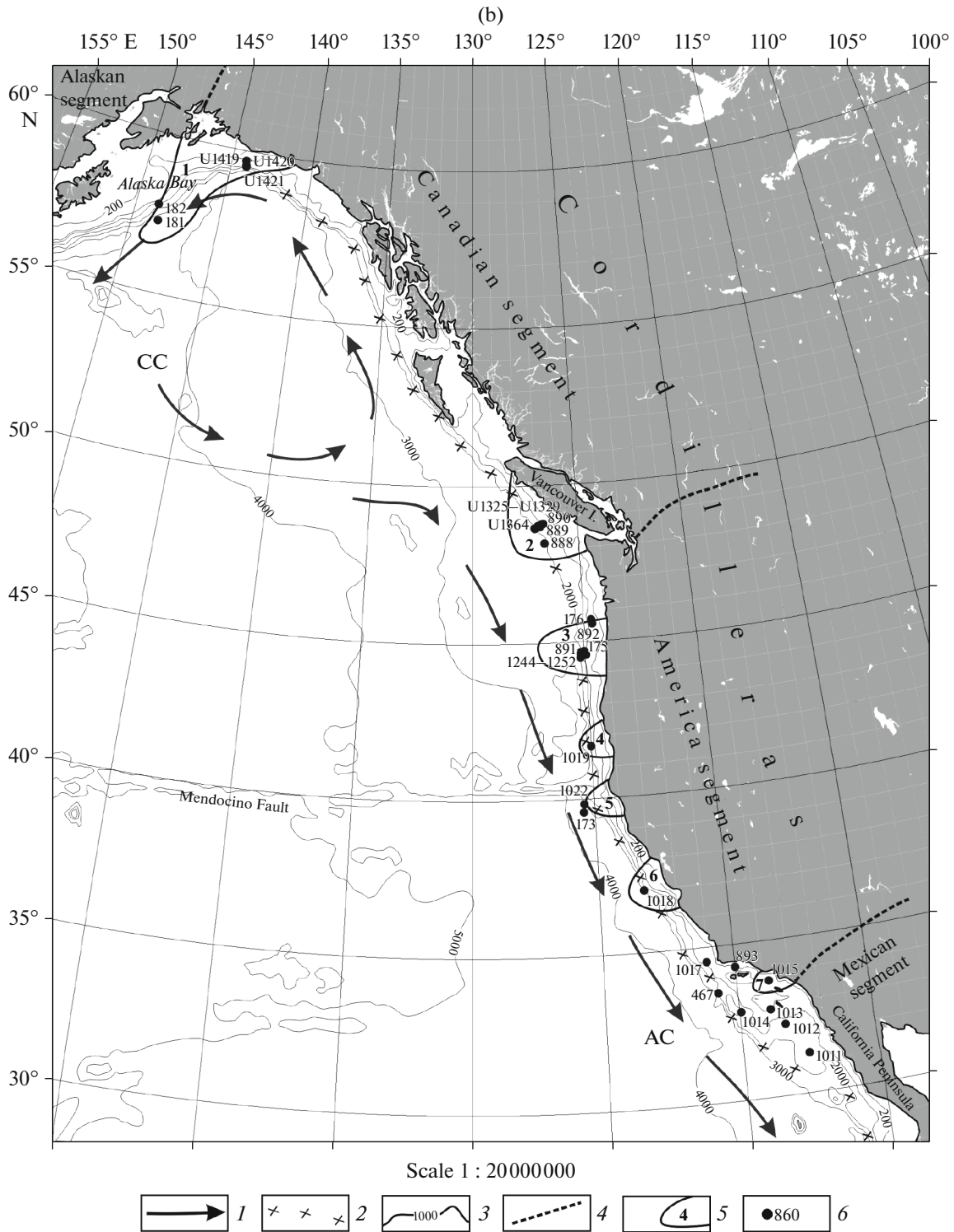


Fig. 1. (Contd.)

In the north of the studied region (from 30° to 61° N), the primary production is much higher owing to the interaction between the cold Californian Current, warm Alaskan Current, and cold Arctic waters (Fig. 1b). The primary production is 600–700 g C/m<sup>2</sup>/y in the area of Californian upwelling, on the continental shelf,

and within Californian Bay (not considered in this paper), and ca. 500 and below 400 g C/m<sup>2</sup>/y above the upper and lower slopes, respectively (Lopes et al., 2010).

The peculiar landforms of submarine margin of the northern area are numerous fans, which are related to

the mountainous rivers on the land and continue as flood riverbeds on the shelf and canyons on the continental slope (Fig. 1b). This area also comprises the Californian borderland with basin system (Santa Monica Basin shown in Fig. 1b is one of them).

On the Cordilleran submarine margin, modern sediments are mainly represented by hemipelagic clays. The Californian Peninsula (including Californian Bay) is surrounded by widespread diatom ooze and clays, while the submarine margin of the southern area is mainly covered by carbonate planktic sediments (McKoy et al., 2003).

## FACTUAL MATERIAL AND METHOD

The following deep-sea drilling legs were carried out in the considered region: DSDP legs nos. 18 (Kulm et al., 1973), 63 (Yeats et al., 1981), 66 (Moore et al., 1982), 67 (Aubouin et al., 1982), 84 (von Huene et al., 1985); ODP legs nos. 146 (Westbrook et al., 1994), 167 (Lyle et al., 1997), 173 (Whitmarsh et al., 1997), and 204 (Tréhu et al., 2007); IODP legs nos. 311 (Riedel et al., 2006), 328 (Davies et al., 2010), 334 (Vannucchi et al., 2012), 341 (Jaeger et al., 2014), and 344 (Harris et al., 2013).

The location of drilled holes is shown in Fig. 1. The lithological, stratigraphic, and physical properties of Pleistocene sediments were taken from the above-mentioned deep-sea drilling reports.

Isobaths shown in Fig. 1 are plotted using the Bathymetric Chart of the World Ocean ([www.gebco.org](http://www.gebco.org)) published in 2004. The lithological map of the modern Pacific sediments was used for comparative–lithological analysis (McKoy et al., 2003). As in the earlier papers of this cycle, the comparative–lithological analysis was carried out using method by Strakhov (1945). The facies–genetic analysis was applied using an approach by Murdmaa (1987), while the volumetric analysis of charts was proposed by Ronov (1949). The sediment volume was recalculated into a dry sediment mass using formula from (Levitán et al., 2013). The Neo- and Eopleistocene lithological–facies maps were compiled using also the boundaries between separate Cordilleran segments and sectors shown in Fig. 1b.

## RESULTS

The maps of factual material (Figs. 1a, 1b) and lithofacies maps with isopachs (Figs. 2a, 2b) on a scale 1 : 20000000 were compiled for the Neo- and Eopleistocene time slices in the azimuthal equal-sized projection. Owing to the extremely large extension of the Cordilleras in submeridional direction and a relatively narrow width of its Pacific margin, all maps were made for two areas: southern (latitudinal boundaries from 80° to 18° N) and northern (latitudinal boundaries from 30° to 61° N). Therefore, the primary descriptions for these two areas will be given separately. No deep-sea drilling holes are available between these areas.

### *The Southern Area*

The Neopleistocene lithofacies map (Fig. 2a) shows the distribution of main sediment types on the submarine margin of the Southern Cordilleras (i.e., on the continental margin of Central America up to the Mid-American deep-water trench). The map has simple appearance: three lithological–facies zones subsequently distinguished along the continental slope span, respectively, its upper, middle, and lower parts. In a first approximation, the upper zone is represented by alternation of diatom clays, hemipelagic clays, and nanoclays. The proportions of the indicated lithologies slightly vary by strike; the thickness over the most part of mapped area exceeds 100 m, and only southeastern part contains a deep-sea fan, the Neopleistocene sequence in the near-shelf part of which is more than 500 m thick. The middle zone is made up of sufficiently monotonous hemipelagic clays, which in the southeast spans not only middle, but also the lower part of the continental slope. The thickness of this sequence usually varies between 50 and 100 m, decreasing toward pelagic region to less than 50 m. The lower lithological–facies zone spans mainly the lower continental slope, southward pinching out. It is composed of diatom clays, which usually contain from 20 to 40% diatoms. The sedimentary sequence sporadically contains single tephra intercalations as well as carbonate nodules. The thickness of these sediments is less than 50 m in the northwestern part of the mapped area and varies from 50 to 100 m in the central part. In general, the thickness of the Neopleistocene sediments decreases downslope toward the pelagic region.

The Eopleistocene lithological–facies map (Fig. 2b) also comprises three lithological–facies zones located from the top downward along the strike of the continental slope. However, as compared to the Neopleistocene, only middle part consists of hemipelagic clays, whose thickness usually varies between 50 and 100 m and decreases to <50 m in the southeast. The upper zone is represented by alternating hemipelagic clays and nanoclays. In the northwest, its thickness usually exceeds 100 m, varying from 50 to 100 m and even less than 50 m in the central part, being more than 250 m in the southeast (in the aforementioned fan). The lower lithological–facies zone consists of the sequence of alternating diatom clays and hemipelagic clays, which usually are from 50 to 100 m thick, but locally does not exceed 50 m. As for the Neopleistocene, the thickness of the Eopleistocene sediments decreases toward pelagic regions. Tephra intercalations are also described in the Eopleistocene sediments.

The calculation of compiled maps using A.B. Ronov volumetric method showed that the sedimentation area in the Neopleistocene accounted for 347 thou. km<sup>2</sup>, while the volume of accumulated sediments is 51.6 thou. km<sup>3</sup>. Hemipelagic clays account for 118.25 thou. km<sup>2</sup> in area; the intercalation of nanoclays, hemipelagic clays, and diatom clays occupies

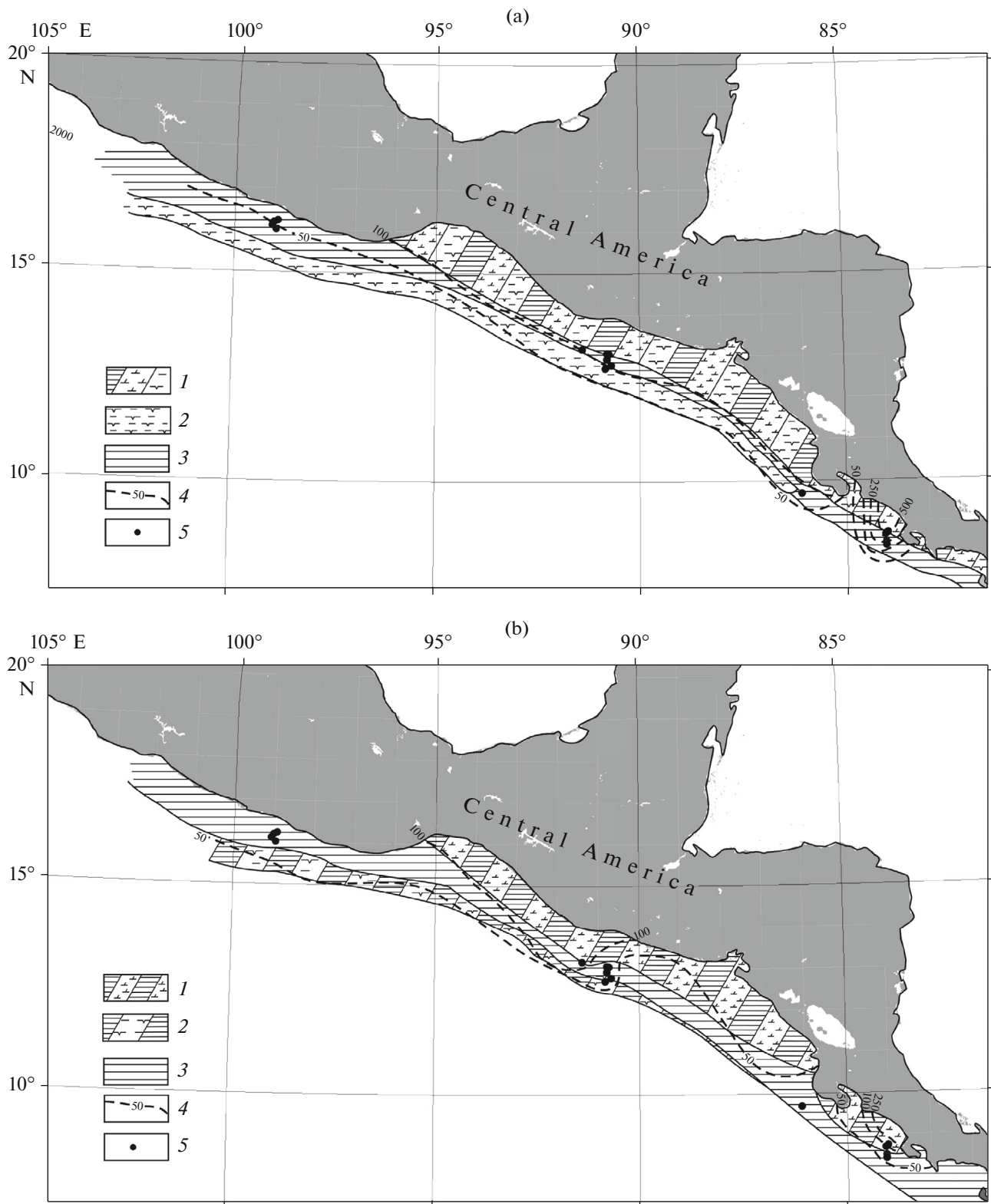


**Fig. 2.** Pleistocene lithological-facies maps for the southern area ((a) Neopleistocene, (b) Eopleistocene). Neopleistocene: (1) alternation of hemipelagic clays, nanoclays, and diatom clays; (2) diatom clays; (3) hemipelagic clays; (4) isopachs (in m); (5) deep-sea drilling holes. Eopleistocene: (1) alternation of hemipelagic clays and nanoclays; (2) alternation of hemipelagic clays and diatom clays; (3) hemipelagic clays; (4) isopachs (in m); (5) deep-sea drilling hole.

**Table 1.** Areas ( $S$ , thou. km<sup>2</sup>) and volumes ( $V$ , thou km<sup>3</sup>) of Pleistocene sediments on the submarine margin of Central America

Bottom sediments	Neopleistocene		Eopleistocene	
	$S$	$V$	$S$	$V$
Hemipelagic clays	274.25	31.59	353.00	15.43
Nanoclays	156.00	8.04	119.50	9.75
Diatom clays	228.75	11.97	58.5	0.49

**Table 2.** Mass of dry sediment ( $M$ , 10<sup>18</sup> g) and of sediment per time unit ( $I$ , 10<sup>18</sup> g/Ma) for Pleistocene sediments on the Central American submarine margin

Bottom sediments	Neopleistocene		Eopleistocene	
	$M$	$I$	$M$	$I$
Hemipelagic clays	23.7	30.0	11.5	11.5
Nanoclays	6.4	8.1	9.4	9.4
Diatom clays	4.5	5.7	0.5	0.5

156.0 thou. km<sup>2</sup>; while diatom clays account for 72.75 thou. km<sup>2</sup>. The hemipelagic clays constitute 61.2%, diatom clays 23.2%, and nanoclays 15.6% of the total volume.

In the Eopleistocene, the hemipelagic clays occupied 175.0 thou. km<sup>2</sup>; alternation of nanoclays and hemipelagic clays, 119.5 thou. km<sup>2</sup>; and alternation of hemipelagic and diatom clays, 58.5 thou. km<sup>2</sup>. The total volume of accumulated sediments is 25.7 thou. km<sup>3</sup>, which includes 60.1% hemipelagic clays, 38.0% nanoclays, and 1.9% diatom clays. Data on areas and volumes of the three main sediment types for the Ne- and Eopleistocene are shown in Table 1. The average thickness of the Neopleistocene and Eopleistocene sediments is 149 and 73 m, respectively.

The subsequent recalculation of data presented in Table 1 into a dry sediment mass and mass of sediments per time unit allowed us to reveal (Table 2) that the mass of hemipelagic and diatom clays and the intensity of their sedimentation were much higher in the Neopleistocene as compared to the Eopleistocene. Nanoclays in the Eopleistocene, in contrast, had slightly higher mass and mass of sediment per time unit.

### The Northern Area

The Neopleistocene lithological–facies map (Fig. 3a) shows the distribution of the main sediment types on the submarine margin of the Northern Cordilleras (i.e., on the North American continental margin up to subduction zone). Based on the obtained data, the considered submarine margin can be subdivided into several segments: (1) margin of the Aleutian arc–Alaska junction zone; (2) Alaskan–Canadian, (3) American,

and (4) Mexican ones. Such subdivision is consistent with a blocked structure of the Cordilleras (Khain, 2001).

The first segment consists mainly of hemipelagic clays with variable amount of ice-rafted debris (IRD). Their thickness varies from 50 to 100 m. Alaska Bay in the Neopleistocene was practically completely occupied by turbidite fan >100 m thick. This is shown in the map (Fig. 3a), however these turbidites at floor depth >3000 m were ignored in calculations with volumetric method.

In the Alaskan–Canadian segment, the shelf consists of alternation of continental diamictites (moraine), IRD-bearing marine hemipelagic clays, and diatom clays. The clay portion of the section corresponds to interglacials, while diamictites, to glacials. Judging from drilling results, the full thickness of the Neopleistocene sequence is more than 1000 m. The continental slope (up to the transect of the southern Vancouver I.) was an arena for the accumulation of IRD-bearing hemipelagic clays reaching from <50 to 50–100 m thick. Large Nitinat fan made up of alternating terrigenous turbidites, hemipelagic clays, and diatom clays is developed seaward of Vancouver I., in Cascadia. In its lower part (older than 0.3 Ma), these slope sediments lie on very compact and deformed terrigenous sediments (mainly, turbidites) of accretionary complex, which is well seen in seismic profiles (Westbrook et al., 1994). Owing to tectonic stacking, the thickness of the rocks during accretion increased and showed significant variations even within very small distances. The sediments contain significant amounts of gas hydrates. In the depocenters, the thickness of the Neopleistocene sediments and rocks can exceed 500 m.

The American segment is represented by the alternation of several fans (described in the section Modern Sedimentation Environments) and fields of IRD-free hemipelagic clays. The fan sequences are usually composed of alternating terrigenous turbidites, hemipelagic clays, and diatom clays. The thickness in the depocenters varies from >500 to 100–250 m. The thickness of fan hemipelagic clays varies from 100–250 to <50 m.

The Mexican segment contains carbonates: coccolithic ooze in alternation with nanoclays and hemipelagic clays in the upper parts of continental slopes and nano- and foraminiferal clays in the middle and lower parts of continental slopes. There are also large fields of hemipelagic clays. The thickness of the Neopleistocene sediments usually is less than 50 m, more rarely, between 50 and 100 m.

The Eopleistocene lithological–facies map (Fig. 3b) sharply differs from the Neopleistocene map. It should be noted that the holes in the northern part of the regions did not go beyond the Neopleistocene. Data on the Quaternary glaciation of Alaska (Hamilton, 1994) and Cordilleras (*Quaternary...*, 2011) suggest the absence of Eopleistocene diamictites on the shelf of the considered submarine margin. As shown in

**Table 3.** Areas ( $S$ , thou. km<sup>2</sup>) and volumes ( $V$ , thou. km<sup>3</sup>) of Pleistocene sediments on the North American submarine margin

Bottom sediments	Neopleistocene		Eopleistocene	
	$S$	$V$	$S$	$V$
Hemipelagic clays	649.7	38.8	610.8	35.1
Nanoclays	133.1	10.3	175.7	7.2
Diatom clays	222.1	9.9	24.4	0.8
Hemipelagic clays with ice-rafted debris	626.0	64.2	679.4	96.5
Terrigenous turbidites	194.9	30.0	85.3	2.8
Diamictites	158.4	16.5	0	0
Nano ooze	81.2	0.6	31.3	0.5

**Table 4.** Mass of dry sediment ( $M$ , 10<sup>18</sup> g) and of sediments per time unit ( $I$ , 10<sup>18</sup> g/Ma) on the North American submarine margin in the Pleistocene

Bottom sediments	Neopleistocene		Eopleistocene	
	$M$	$I$	$M$	$I$
Hemipelagic clays	32.3	40.9	33.8	33.8
Nanoclays	7.7	9.8	6.5	6.5
Diatom clays	7.4	9.4	0.7	0.7
Hemipelagic clays with ice-rafted debris	53.7	68.0	82.5	82.5
Terrigenous turbidites	29.5	37.3	2.7	2.7
Diamictites	27.9	35.3	0	0
Nano ooze	0.5	0.6	0.5	0.5

Fig. 3b, the shelves and areas of continental slopes in the Alaskan–Canadian segment presumably accumulated hemipelagic clays with dispersed ice-rafted detritus. Their thickness likely varied between 100 and 250 m, rarely exceeding these values, and sometimes decreasing to <50 m. Small occurrence of diatom clays is described at a latitude of Vancouver I. Noteworthy is the absence of terrigenous turbidite fields.

In the American segment, two Eopleistocene lithological-facies zones can be distinguished. One zone spans shelf and upper slope and consists of alternating terrigenous turbidites, hemipelagic clays, and nanoclays. This zone includes only one well developed fan (Fig. 3b), the thickness of which exceeds 250 m in the depocenter. The thickness of the considered sequence is usually ca. 100 m. The other lithological–facies zone spanning the middle and lower parts of the continental slope accumulated sufficiently homogenous hemipelagic clays <50 m thick in the Eopleistocene.

The northern part of the Mexican segment is occupied by hemipelagic clays and (downslope) by alternation of foraminiferal–coccolithic and diatom–coccolithic clays. A small field of nanoclays is located southerly, while the southern part of the segment is occupied by alternating hemipelagic clays and nanoclays. In this area, the thickness of Eopleistocene sediments varies from 50 to 100 m, locally decreasing to <50 m.

Processing of compiled maps using A.B. Ronov volumetric method showed that the Neopleistocene sedimentation area was 1369.1 thou. km<sup>2</sup> in area and 170.3 thou. km<sup>3</sup> in volume. This area included (in thou. km<sup>2</sup>) 457.8 hemipelagic clays; 424.9 IRD-bearing hemipelagic clays; 47.4 nanoclays, and 41.5 terrigenous turbidites. The remained sedimentation area is represented by diverse types of alternation shown in the map (Fig. 3a). The IRD-bearing hemipelagic clays, hemipelagic clays, terrigenous turbidites, diamictites, nanoclays, diatom clays, and nano ooze account for 37.7, 22.8, 17.6, 9.7, 6.1, 5.8, and 0.4%, respectively, of the total volume.

In the Eopleistocene, hemipelagic clays occupied 418.1 thou. km<sup>2</sup>; hemipelagic clays, including ice-rafted detritus (IRD), 679.4 thou. km<sup>2</sup>; and nanoclays, 30.5 thou. km<sup>2</sup>. The remained sedimentation area is represented by diverse alternation types, shown in the map (Fig. 3b). The total volume of the sediments is 143.0 thou. km<sup>3</sup>, including IRD-bearing hemipelagic clays (67.5%), hemipelagic clays (24.5%), nanoclays (5.0%), terrigenous turbidites (2.0%), diatom clays (0.6%), nano ooze (0.3%), and diamictites (0%).

Data on the distribution area and volumes of the indicated three main sediment types of the Neo- and Eopleistocene are shown in Table 3. The average

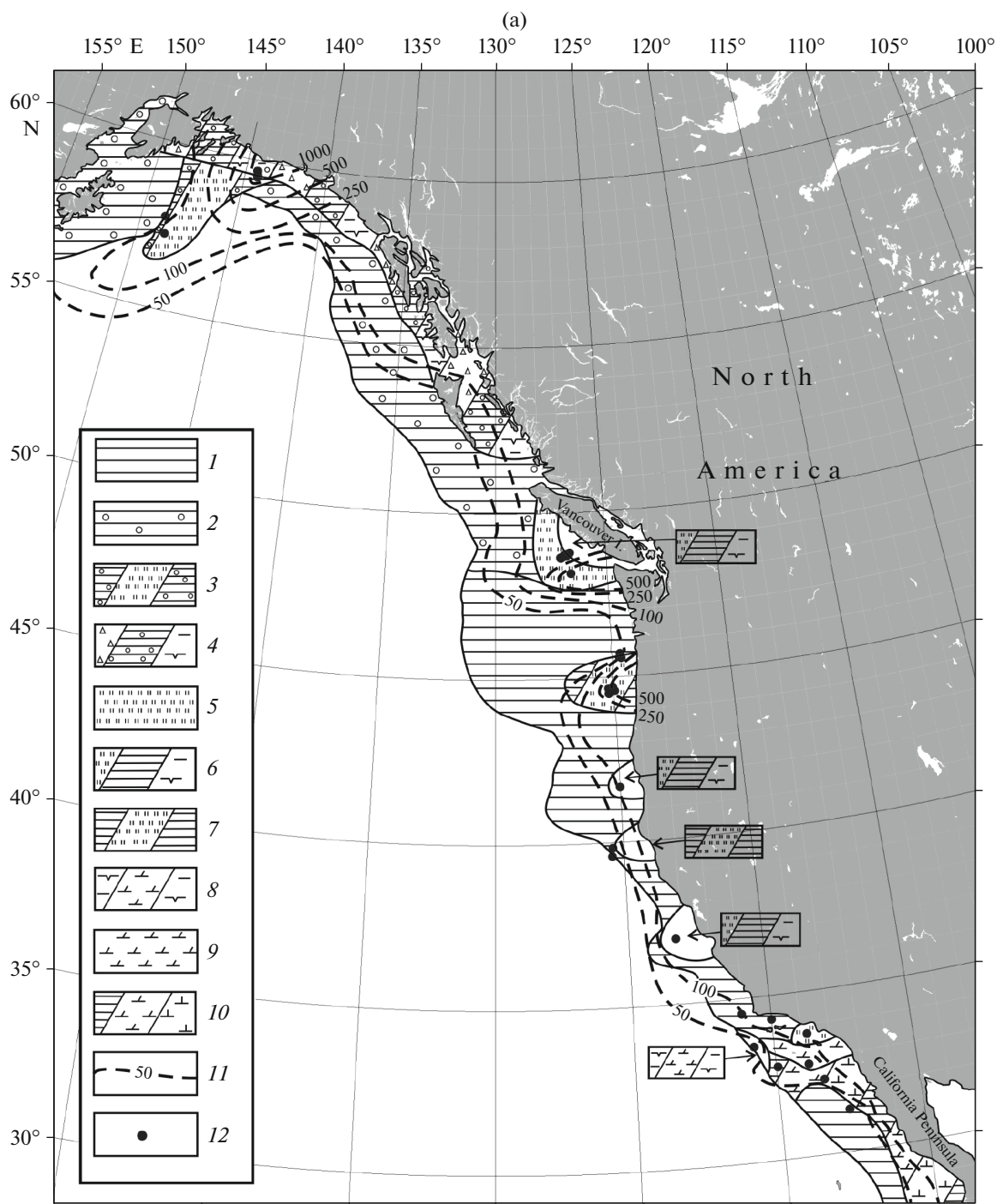


**Fig. 3.** Pleistocene lithological-facies maps for the northern area ((a) Neopleistocene; (b) Eopleistocene). Neopleistocene: (1) Hemipelagic clays; (2) hemipelagic clays with ice-rafted detritus; (3) alternation of terrigenous turbidites and hemipelagic clays with ice-rafted detritus; (4) alternation of diamictites, pelagic clays with material of ice-rafted debris and diatom clays; (5) terrigenous turbidites; (6) alternation of terrigenous turbidites, hemipelagic clays, and diatom clays; (7) alternation of terrigenous turbidites and hemipelagic clays; (8) alternation of diatom clays and nanoclays; (9) nanoclays; (10) alternation of coccolithic ooze, nanoclays, and hemipelagic clays; (11) isopachs (in m); (12) deep-sea drilling hole. Eopleistocene: (1) hemipelagic clays; (2) hemipelagic clays with ice-rafted detritus; (3) diatom clays; (4) alternation of terrigenous turbidites, hemipelagic clays, and nanoclays; (5) alternation of terrigenous turbidites and hemipelagic clays; (6) alternation of hemipelagic clays and diatom clays; (7) alternation of coccolithic ooze and nanoclays; (8) nanoclays; (9) alternation of foraminiferal nanoclays and diatom nanoclays; (10) alternation of nanoclays and hemipelagic clays; (11) isopachs (inm); (12) deep-sea drilling holes.



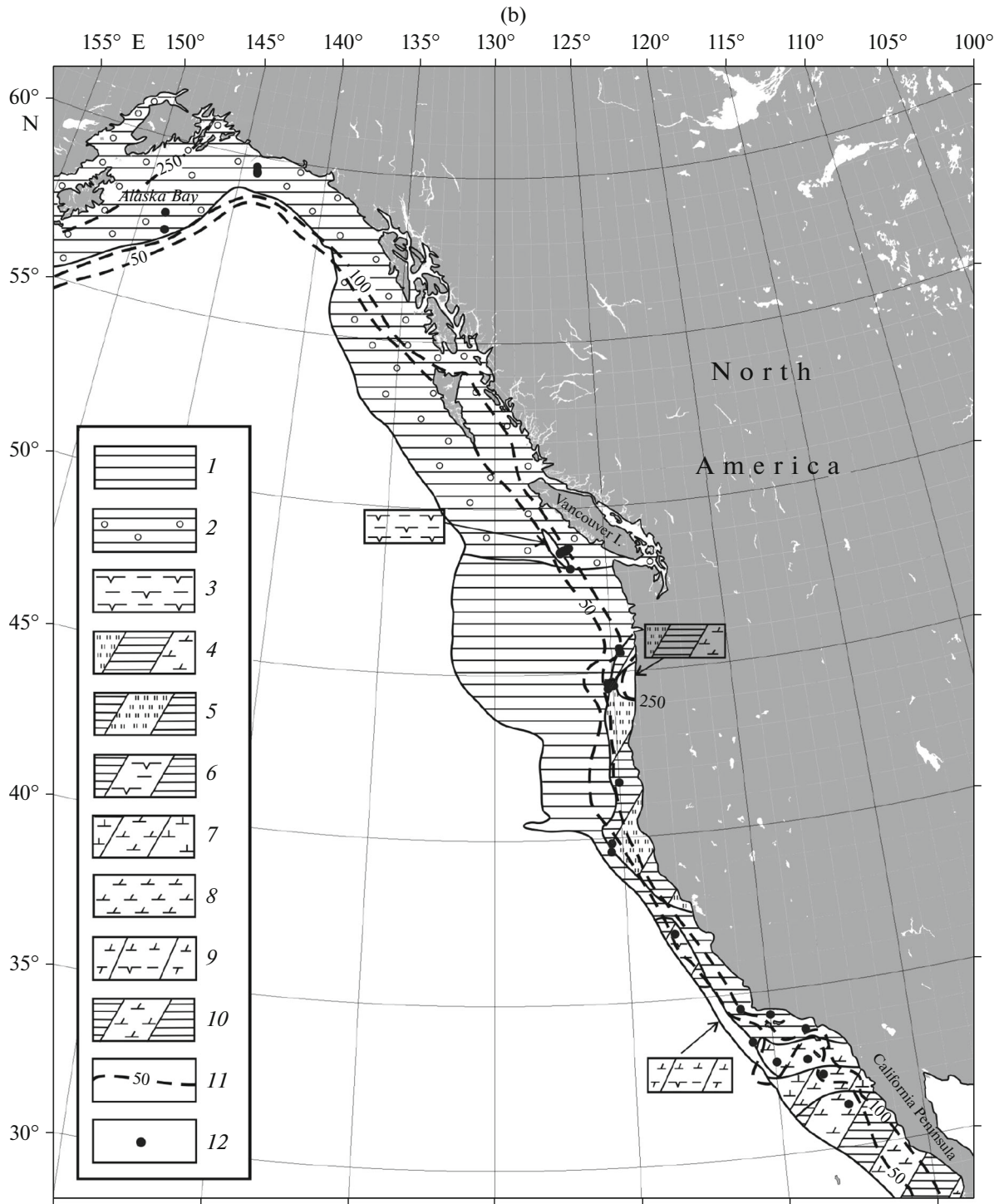


Fig. 3. (Contd.)

thickness of the Neopleistocene and Eopleistocene sediments is 124 and 105 m, respectively.

The recalculation of data presented in Table 3 into a dry sediment and a mass of sediment per time unit revealed the following tendencies (Table 4): (1) the predominance of terrigenous turbidites and diamictites, diatom clays, and nanoclays in the Neopleisto-

cene as compared to the Eopleistocene; (2) the predominance of hemipelagic clays and IRD-bearing hemipelagic clays in the Eopleistocene as compared to the Neopleistocene; (3) more intense accumulation of sediments in the Neopleistocene compared to the Eopleistocene, except for IRD-bearing hemipelagic clays; (4) the ratio of the total intensity of accumulation

of terrigenous sediments in the Neopleistocene to that of the Eopleistocene ( $IQ_{2+3}/IQ_1$ ) accounted for 1.5.

## DISCUSSION

Judging from obtained results, the Pleistocene was marked by a significant change of the facies structure of sediments and their quantitative parameters on the submarine Cordilleran margins. Owing to the intensification of Cordilleras and Alaska glaciations, the mountainous glaciers in the north of the considered area increased in volume, descent, and reached shelf, which follows from the development of thick diamictite sequences. In addition to the intensification of glaciation, the Pleistocene was also characterized by the elevated amplitude of tectonic movements, which led to the sharp increase of terrigenous flux in the Neopleistocene, and, respectively, formation of numerous fans and turbid flows. Climatic changes facilitated vertical circulation, including Californian upwelling in the Neopleistocene.

The combination of data from the southern and northern areas indicates that the intensity of sediment accumulation on the Cordilleran submarine margin in the Neopleistocene as compared to the Eopleistocene increased by 2.6 times for the terrigenous material, by 2.0 times for carbonate sediments, and by 12.6 times for siliceous sediments. Obtained trends correspond to the general tendencies revealed previously for the Pacific pelagic sediments (Levitan et al., 2013, Levitan, 2016).

## ACKNOWLEDGMENTS

This paper was financially supported by the Russian Foundation for Basic Research (project no. 17-05-00157) and by the Presidium of the Russian Academy of Sciences (program no. I.49P). The work was performed in the framework of the State Task no. 0137-2016-0008.

## REFERENCES

- J. Aubouin, R. von Huene, et al. *Init. Repts. DSDP 67*, 1982.
- W. H. Berger, K. Fisher, C. Lai, and G. Wu, "Ocean productivity and organic carbon flux. Part I. Overview and maps of primary production and export production," (Univ. of California, San Diego, SIO Reference 1987), pp. 97–130.
- J. Clague, J. R. Harper, R. J. Hebda, and D. E. Howes, "Late Quaternary sea levels and crustal movements, coastal British Columbia," *Can. J. Earth Sci.* **19**, 597–618 (1982).
- E. Davies, M. Malone et al., *Proc. IODP, Init. Repts.* 328, (2010).
- F. M. Gradstein, J. G. Ogg, and A. G. Smith, *A Geologic Time Scale 2004* (Cambridge Univ. Press, 2004).
- T. D. Hamilton, "Late Cenozoic glaciation of Alaska," *The Geology of Alaska*, Ed. by G. Plafker and H.C. Berg (GSA, 1994), pp. 813–844.
- R. N. Harris, A. Sakaguchi, K. Petronotis, et al., *Proc. IODP, Init. Repts.* **344**, (2013).
- V. M. Jaeger, S. P. S. Gulick, L. G. LeVay, et al., *Proc. IODP, Init. Repts.* **341**, (2014).

- V. E. Khain, *Tectonics of Continents and Oceans* (Nauchnyi Mir, Moscow, 2001) [in Russian].
- Kulm L.D., von Huene R. et al., *Init. Repts. DSDP 18*, (1973).
- M. A. Levitan, "Comparative analysis of pelagic Pleistocene silica accumulation in the Pacific and Indian oceans," *Geochem. Int.* **54** (3), 257–265 (2016).
- M. A. Levitan, A. N. Balukhovskiy, T. A. Antonova, and T. N. Gelvi, "Quantitative parameters of Pleistocene pelagic sedimentation in the Pacific ocean," *Geochem. Int.* **51** (5), 345–352 (2013).
- M. A. Levitan, T. N. Gelvi, K. V. Syromyatnikov, and K. D. Chekan, "Facies structure and quantitative parameters of Pleistocene sediments of the Bering Sea," *Geochem. Int.* **56**(4), 304–317 (2018a).
- M. A. Levitan, T. A. Antonova, L. G. Domaratskaya, A. V. Kol'tsova, and K. V. Syromyatnikov, "Facies structure and quantitative parameters of Pleistocene sediments of the Sea of Japan," *Byul. Komis. Izuch. Chetvertichn. Perioda*, No. 76, 135–142 (2018b).
- M. A. Levitan, T. A. Antonova, A. V. Kol'tsova, and L. G. Domaratskaya, "Facies structure and quantitative parameters of Pleistocene sediments of China seas," *Byul. Komis. Izuch. Chetvertichn. Perioda*, No. 76, 143–156 (2018c).
- C. Lopes, A. C. Mix, and F. Abrantes, "Environmental controls of diatom species in the northeast Pacific," *Palaeogeogr., Palaeoclimatol., Palaeoecol.* **297** (1), 188–200 (2010).
- M. Lyle, I. Koizumi, C. Richter, et al., *Proc. ODP, Init. Repts.* **167**, (1997).
- F. H. McKoy, T. R. Suint, and D. Z. Piper, "Types of bottom sediments," *International Geological-Geophysical Atlas of the Pacific Ocean*, Ed. by G. B. Udintsev (Moscow-St. Petersburg, 2003), pp. 114–115 [in Russian].
- J. C. Moore, J. S. Watkins, et al., *Init. Repts. DSDP 66*, (1982).
- I. O. Murdmaa, *Oceanic Facies* (Nauka, Moscow, 1987) [in Russian].
- Quaternary Glaciations—Extent and Chronology*, Ed. by J. Ehlers, P. L. Gibbard, and P. G. Hughes (Elsevier, Amsterdam, 2011), vol. 15.
- M. Riedel, M. Collett, M. J. Malone, et al., *Proc. IODP, Init. Repts.* **311**, (2006).
- A. B. Ronov, "History of sedimentation and fluctuations of the European USSR," *Tr. Geofiz. Inst.*, No. 3 (1949).
- N. M. Strakhov, "Comparative—lithological direction and its nearest tasks," *Byul. Mosk. O-va. Isp. Prir., Otd. Geol.* **20** (3/4), 34–48 (1945).
- A. M. Tréhu, G. Bohrmann, F. Rack, et al., *Proc. ODP, Init. Repts.* **204**, (2007).
- V. G. Trifonov, and S. Yu. Sokolov, "On the way to plate tectonics," *Vestn. Ross. Akad. Nauk* **85** (7), 605–615 (2015).
- P. Vannucchi, K. Ujiie, A. Malinverno, et al., *Proc. IODP, Init. Repts.* **334**, (2012).
- R. Von Huene, J. Aubouin, et al., *Init. Repts. DSDP 84*, (1985).
- G. K. Westbrook, B. Carson, R. J. Musgrave, et al., *Proc. ODP, Init. Repts.* **146** (1), (1994).
- R. Whitmarsh, B. M.-O. Beslier, P. J. Wallace, et al., *Proc. ODP, Init. Repts.* **173**, (1997).
- www.gebco.org (2004)
- R. S. Yeats, B. U. Haq, et al., *Init. Repts. DSDP 63*, (1981).

*Translated by M. Bogina*